OPEN ACCESS Freely available online

AFM Applied Functional Materials

ISSN 2737-5323
Volume 2, Issue 4
https://www.iikii.com.sg/journal/AFM
Applied Functional Materials

Article

Molecular-Dynamical Investigation of Thermomechanical Properties of Spherical Solid and Hollow Nickel Nanopowder during Laser Additive Manufacturing Process

Ling-Feng Lai [1], Yu-Chen Su [2], Chun-Ming Chang [3], Kuei-Shu Hsu [4], Deng-Maw Lu [1], and Jian-Ming Lu [5,*]

[1] Department of Mechanical Engineering, Southern Taiwan University of Science and Technology, Taiwan; da71y201@stust.edu.tw, dmlu@stust.edu.tw
[2] Department of Civil Engineering, National Central University, Taiwan; ycsu@ncu.edu.tw
[3] Taiwan Instrument Research Institute, National Applied Research Laboratories, Taiwan; gmp@narlabs.org.tw
[4] Department of Recreation and Health Care Management, Chia Nan University of Pharmacy & Science, Taiwan; fkshsu888@mail.cnu.edu.tw
[5] National Center for High-Performance Computing, National Applied Research Laboratories, Taiwan;
* Correspondence: 0403817@narlabs.org.tw;

Received: Nov 3, 2022; **Accepted:** Dec 3, 2022; **Published:** Dec 30, 2022

Abstract: Molecular dynamics (MD) simulation with the embedded-atom method (EAM)/alloy potential is used to investigate the property of the nanoscale hollow spherical Nickel (Ni) powder during the laser additive manufacturing (AM) process. The thermomechanical properties of the Ni nanopowder is also explored (1) at room temperature and (2) from room temperature to the melting temperature during laser AM of powder bed fusion. As a result, the optimum parameters for the laser AM process are proposed. The optimal coalescence temperature of the nanoscale hollow spherical Ni powder is in the range between 980 and 1421K, while the melting temperature is in the range between 1320 and 1470 K. The coalescence and melting temperatures are lower than the melting point of Ni (1728 K).

Keywords: molecular dynamics, nanoscale, additive manufacturing, coalescence, melting

1. Introduction

Laser AM is used in three-dimensional printing (3DP) [1−3]. Laser AM for metals is mostly used in the manufacturing process for aerospace, machinery, biomedicine supplies, and so on to print implants, prosthetics, and medical devices. As Ni has high ductility, corrosion resistance, chemical activity, and hardness, it is often used in electroplating, steel alloy, dyes, catalysts, batteries, and others. In this present study, the thermomechanical property of the spherical solid and hollow Ni nanopowders such as the coalescence temperature and melting temperature are investigated using MD simulation [2] under different conditions during the Laser AM process.

2. Methodology

2.1. MD simulation

MD is used to calculate the motion of molecules in the atomic system. Large-scale atomic and molecular massively parallel simulator (LAMMPS) [4-5] is one of the open-source MD simulation programs. In this study, LAMMPS is used to simulate the structure, thermodynamics, dynamics, and force of the nanoscale hollow spherical Ni powder. Using the LAMMPS, the thermomechanical property of the Ni powders is analyzed at the coalescence temperature and melting temperature.

2.2. Nanoscale spherical Ni model

Solid and hollow Ni nanoparticle are simulated by LAMMPS with the parameters in the non-periodic boundary condition. The NVT ensemble (canonical ensemble) for the initial structure of Ni is the face-centered cubic (FCC) crystal structure. The disordered atomic structure is set on the outer surface of the Ni nanoparticle, and the space of the simulation is several times larger than that of solid and hollow Ni nanoparticle. The initial gap between the Ni nanoparticle is set to 5 Å, and the lattice constant is set to 3.9201

Å, The nanoparticle sizes of the Ni nanoparticle are 16, 20, and 24a which are 3 different nanoparticle sizes for solid and hollow Ni powders. The parameters for 6 groups are shown in Table 1 and Fig. 1.

Table 1. Parameters of solid and hollow Ni powder model in nanoscale

D1	D2	Solid (Number of atoms)	Hollow (Number of atoms)
16a	**16a**	17,718	15,056
16a	**20a**	25,346	20,696
16a	**24a**	37,486	27,836
20a	**20a**	33,514	26,336
20a	**24a**	45,654	33,476
24a	**24a**	57,794	40,616

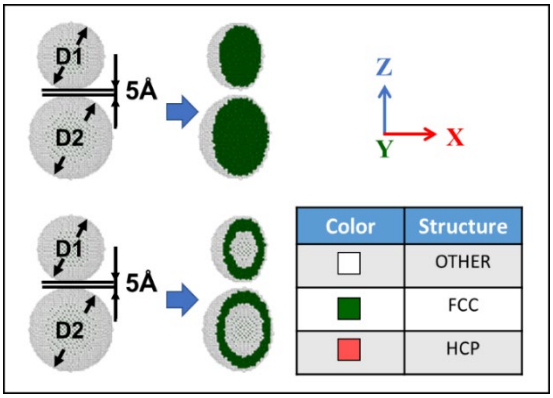

Fig. 1. Cross-sectional view of the nanoscale model for solid (upper) and hollow (lower) Ni powder.

2.3. Common neighbor analysis

The EAM/alloy potential function is used to describe the atomic interaction, interactive force, position, displacement trajectory, and electron density of the solid and hollow Ni powder with the wave function [6–8]. In the EAM/alloy potential, the energy of each atom is embedded in the local electron density energy [8]. Common neighbor analysis (CNA) is used to visualize and explore the internal lattice structure of the solid and hollow Ni powder at each time step and the change and occupation of the structure by distinguishing different colors [9,10]. The gyration radius (R_g) is calculated to simulate the root mean square distance from the center of mass of each atom in the Ni powder [9,10]. (Eq. (1))

$$R_g^2 = \frac{1}{M}\sum_i m_i(r_i - r_{cm})^2 \quad (1)$$

where $\boldsymbol{M}$ is the total mass of the simulated environment, $\boldsymbol{r_{cm}}$ is the center of mass of the atom, $\boldsymbol{r}$ is the position of each atom in the nanopowder, and all atoms in the simulated environment space are set to the subscript $\boldsymbol{i}$.

Mean square displacement (MSD) is calculated to simulate the initial position, the displaced position, and the average distance of the solid and hollow spherical Ni nanopowder (Eq. (2)) [9,10].

$$MSD = \frac{1}{N}\sum_i [r_i(t) - r_i(0)]^2 \quad (2)$$

where $\boldsymbol{N}$ is the total number of the simulated environment, t is the time, $\boldsymbol{r}$ is the position of each atom in the powder, and the subscript $\boldsymbol{i}$ is all atoms in the simulated environment.

3. Results and Analysis

3.1. Spherical solid Ni nanopowder model

3.1.1. Thermal equilibration at 300 K

LAMMPS is used to simulate the force, thermodynamics, atomic mechanics, and internal structure change of the spherical solid Ni nanopowder at room temperature (300K). Fig. 2 shows the four scales ((a), (b), (c), and (d)). The gap of the spherical solid Ni nanopowder without being heated at Point (a) is kept at a distance of 5 Å, a gyration radius of 41.17Å, and a neck width of 0Å. The FCC accounts for 80.44%, while the hexagonal close packing structure (HCP) accounts for 0%, and the others account for 19.56%. At Point (b), the Ni nanopowders contact each other due to the small size effect. The radius of gyration is 41.17Å, and the neck width is 27.97Å, and FCC, HCP, and the others accounts 80.21%, 0%, and 19.79%, respectively. At Point (c), the radius of gyration is 41.17Å, and the neck width 29.30Å with 78.68% of FCC and 0.67%, of HCP. The other structures account for 20.65%. At Point (d), the radius of gyration is 41.16Å, the neck width is 33.72Å, and FCC, HCP, and other structures 81.18%, 0%, and 18.82%, respectively.

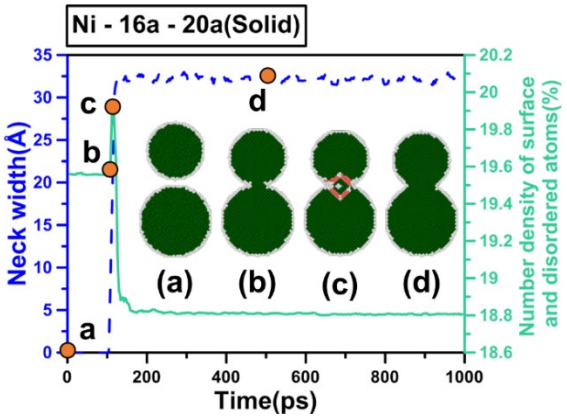

Fig. 2. Change in neck width and density curve of spherical solid Ni nanoparticle of 16−20a sintered by laser at 0.25K/ps at 300 and 1800 K.

It is observed that the overall structural state of the Ni nanopowder is stable from Points A to C (Fig. 3). The spherical solid Ni nanopowder under the heating of laser sintering is stable from Points C to D. This indicates that the nanopowders coalesce together. The internal structure of the spherical solid Ni nanopowder gradually changes from Point D to E while the atomic lattice structure changes drastically due to melting. After Point E, the spherical solid Ni nanopowder melts in the complete melting region.

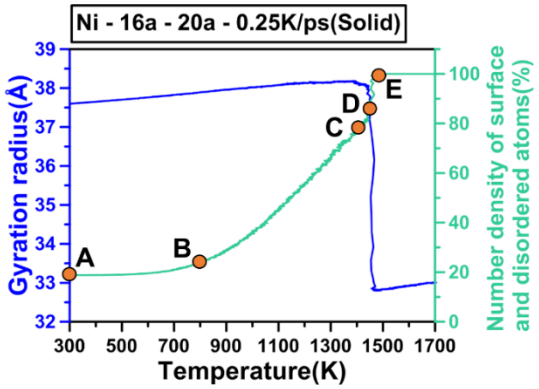

Fig. 3. Change in Gyration radius and density curve of spherical solid Ni nanoparticle of 16−20a sintered by laser at heating rates of 0.25K/ps at 300 and 1800 K.

3.1.2. Laser sintering

The distance of the atomic displacement trajectory of the spherical solid Ni nanopowder becomes the largest under laser sintering heating at a heating rate of 0.25K/ps as shown in Fig. 4. The nanoscale coalescence temperature of the spherical solid Ni nanopowder is in the range between 1287 and 1515K (Fig. 5), and nanoscale melting temperature of spherical solid Ni nanopowder is in the range between 1420 and 1568K (Fig. 6).

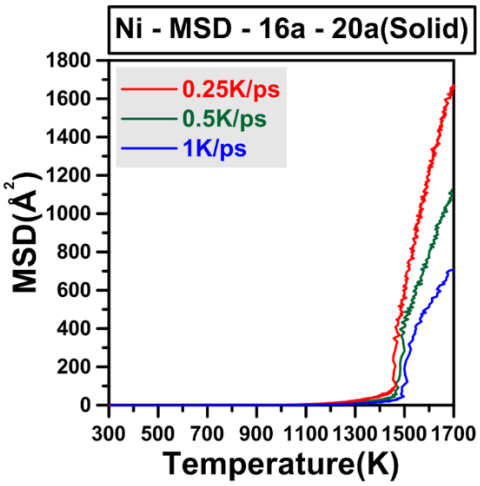

Fig. 4. MSDs of spherical solid Ni nanoparticles at different heating rates of 0.25, 0.5, and 1K/ps and different temperatures between 300 and 1800K.

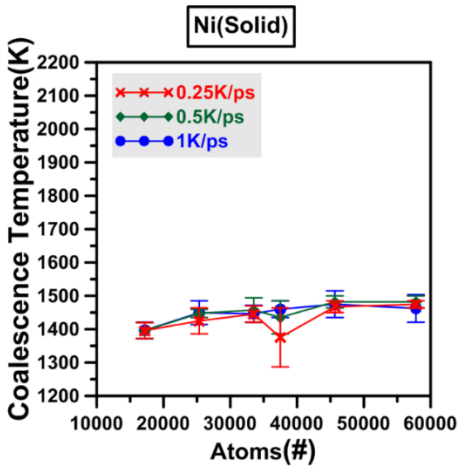

Fig. 5. Coalescence temperature as a function of the number of atoms (10000−60000) of spherical solid Ni nanoparticles at 3 laser heating rates of 0.25, 0.5, and 1K/ps.

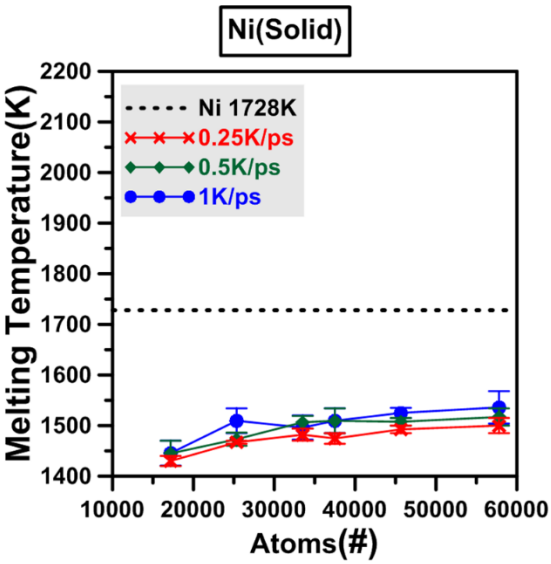

Fig. 6. Melting temperature as a function of the number of atoms (10000−60000) of spherical solid Ni nanoparticles at 3 laser heating rates of 0.25, 0.5, and 1K/ps. The dotted line is for the melting point of Ni, 1728 K.

3.2. Hollow spherical Ni nanopowder model

3.2.1. Thermal equilibration at 300 K

Spherical hollow Ni nanopowders maintain an initial distance of 5 Å. The gyration radius is 47.81Å, the neck width is 0Å, and FCC, HCP, and other structures account for 67.14%, 0%, and 32.86% at Point a (Fig. 7). At Point b, the spherical hollow Ni nanopowder is in the solid sintering process due to a small effect. Spherical hollow Ni nanopowder particles no longer maintain the distance but contact with each other. The gyration radius is 47.81Å, the neck width is 28.15Å, FCC accounts for 67.13%, HCP accounts for 0%, and the others account for 32.87%. At Point c, the gyration radius is 47.81Å, the neck width is 38.61Å, and FCC, HCP, and other structures account for 66.10%, 0.54%, and 33.36%, respectively. At Point d, the structure state of the spherical hollow Ni nanopowder is in equilibrium with the gyration radius of 47.72Å, the neck width of 37Å is. FCC accounts for 67.77%, HCP accounts for 0%, and the other structures account for 32.23%.

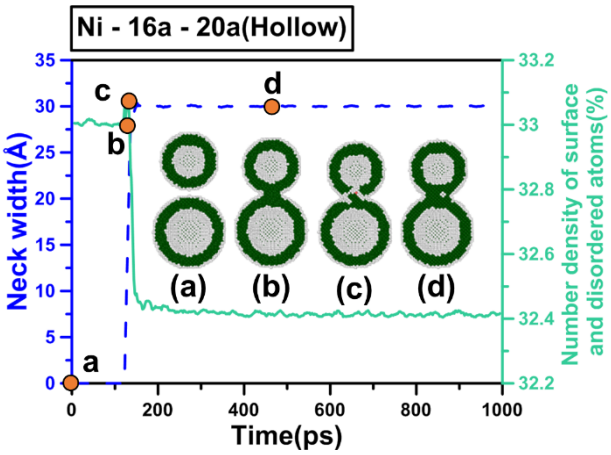

Fig. 7. Change in neck width and density curve of spherical hollow solid Ni nanoparticle of 16−20a sintered by laser at 0.25K/ps at 300 and 1800 K.

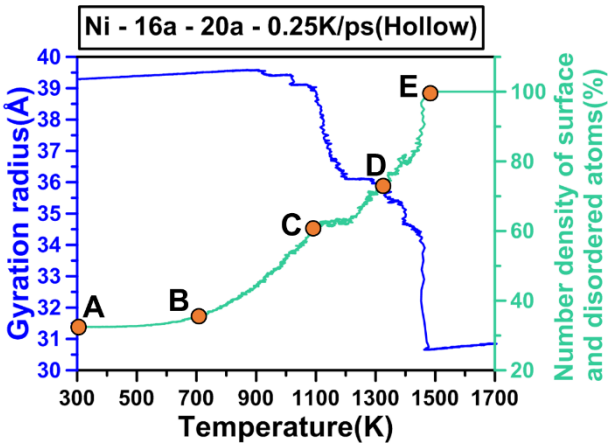

Fig. 8. Change in neck width and density curve of spherical hollow solid Ni nanoparticle of 16−20a sintered by laser at 0.25K/ps at 300 and 1800 K.

3.2.2. Laser sintering

The laser sintering region is divided into 4 sections, which are relatively stable (from Points A to C in Fig. 8). The overall structure of the spherical hollow Ni nanopowder is stable. From Points C to D in Fig. 8, the spherical hollow Ni nanopowders coalesce together due to being heated under laser sintering. The internal structure of the spherical hollow Ni nanopowder begins to melt from Point D, and completely melts after Point E of Fig. 8. In Figs. 4 and 9, the trajectory distance of the atomic displacement of the spherical hollow Ni nanopowder becomes the largest under laser sintering at the heating rate of 0.25K/ps. The nanoscale coalescence temperature of the spherical solid Ni nanopowder is in the range of 1287 and 1515K (Fig. 10), while that of the spherical hollow Ni nanopowder is in the range of 1420 and 1568 K (Fig. 11). Fig. 8 shows that when being heated by the laser sintering, the melting

temperature of the hollow spherical Ni nanopowder is in the range of 980 and1421 K. Fig. 9 shows that the melting temperature is in the range of 1320 and 1470K which is shown by the cut-off radius and potential energy function.

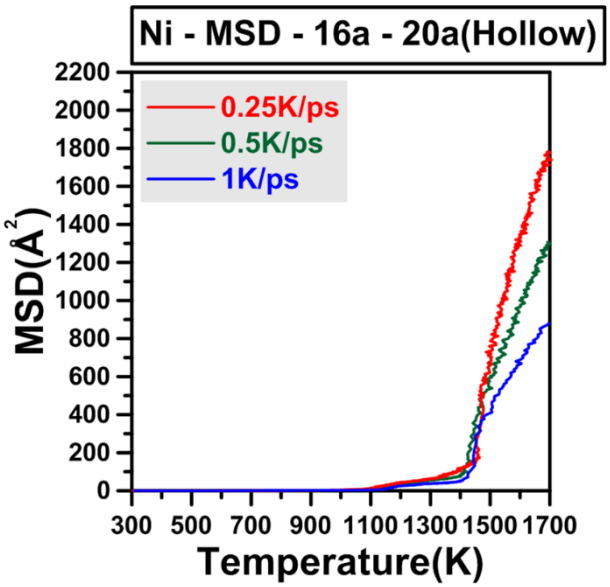

Fig. 9. MSDs of spherical hollow Ni nanoparticles at different heating rates of 0.25, 0.5, and 1K/ps and different temperatures between 300 and 1700K.

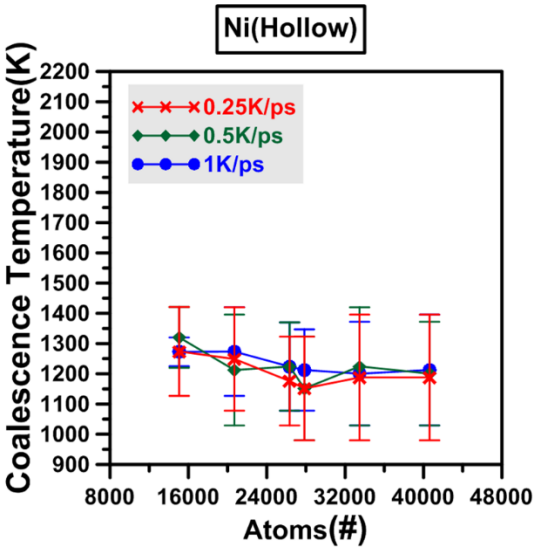

Fig. 10. Coalescence temperature as a function of the number of atoms (10000−50000) of spherical solid Ni nanoparticles at 3 laser heating rates of 0.25, 0.5, and 1K/ps.

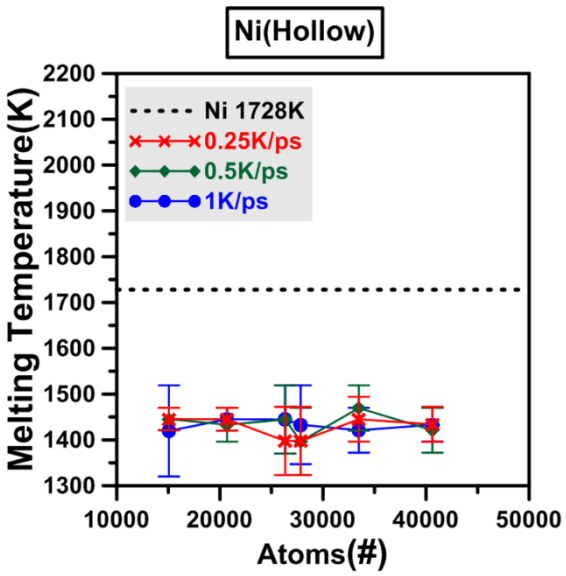

Fig. 11. Melting temperature as a function of the number of atoms (10000−50000) of spherical hollow Ni nanoparticles at 3 laser heating rates of 0.25, 0.5, and 1K/ps. The dotted line is for the melting point of Ni, 1728 K.

4. Conclusions

As Ni has high ductility, corrosion resistance, chemical activity, and hardness, it is mainly used in electroplating, steel alloy, dyes, catalysts, batteries, and others. Thus, it is important to understand the thermomechanical properties of the spherical Ni nanopowder under different conditions during the laser AM process which is used to manufacture it. In this study, coalescence temperature and melting temperature are also determined using MD simulation. In this present study. The coalescence temperature is in the range of 980 and 1421K and of 1287 and 1515K for the spherical solid and hollow Ni powders. The melting temperature is in the range of 1420 and 1568K and 980 and 1421 K. for the spherical solid and hollow Ni nanopowders. The lower the heating rate, the better the diffusive effect of Ni atoms. The solid-state sintering of the spherical hollow Ni nanoparticle occurs at 300K. The coalescence temperature and melting temperature of the spherical solid and hollow Ni nanopowders are lower than the melting point of Ni metal (1728 K) [9-11].

Author Contributions: conceptualization, Ling-Feng Lai, Deng-Maw Lu, and Jian-Ming Lu; methodology, Deng-Maw Lu, Kuei-Shu Hsu, and Jian-Ming Lu; software, Ling-Feng Lai and Jian-Ming Lu; validation, Ling-Feng Lai; formal analysis, Ling-Feng Lai and Jian-Ming Lu; investigation, Ling-Feng Lai, Deng-Maw Lu, Kuei-Shu Hsu, and Jian-Ming Lu; resources, Yu-Chen Su, Deng-Maw Lu, and Jian-Ming Lu; data curation, Ling-Feng Lai and Jian-Ming Lu.; writing—original draft preparation, Ling-Feng Lai, and Jian-Ming Lu; writing—review and editing, Yu-Chen Su, Chun-Ming Chang, Deng-Maw Lu, Kuei-Shu Hsu, and Jian-Ming Lu; visualization, Ling-Feng Lai, Deng-Maw Lu, and Jian-Ming Lu; supervision, Deng-Maw Lu and Jian-Ming Lu.

Funding: We would like to thank the the funding from the Ministry of Science and Technology of Taiwan under the contract number MOST 110-2222-E-008-009-MY2.

Acknowledgments: The authors grateful thank the computational time, resources, and facilities from the National Center for High-Performance Computing of National Applied Research Laboratories of Taiwan. We also thank Dr. Chun-Ming Chang, Yu-Wen Chiang, Yu-Sheng Lin, Chi-Wen Yang, Chao-Chen Li, Chi-Hung Wang, and Yow-Shiuan Liaw for their efforts.

Conflicts of Interest: The authors declare no conflict of interest.

References

1. Frazier, W.E. Metal additive manufacturing: a review. *Journal of Materials Engineering and Performance*. **2014**, *23*, 1917–1928.
2. Conner, B.P.; Manogharan, G.P.; Martof, A.N.; Rodomsky, L.M.; Rodomsky, C.M.; Jordan, D.C.; Limperos, J.W. Making sense of 3-Dprinting: Creating a map of additive manufacturing products and services. *Additive Manufacturing*. **2014**, *1*, 64–76.
3. Vaezi, M.; Seitz, H.; Yang, A. A review on 3D micro-additivemanufacturing technologies. *The International Journal of Advanced Manufacturing Technology*. **2013**, *67*, 1721–1754.
4. Jiang, S.; Zhang, Y.; Gan, Y.; Chen, Z.; Peng, H. Molecular dynamics study of neck growth in laser sintering of hollow silver nanoparticles with different heating rates. *J. Phys. D: Appl. Phys*. **2013**, *46*, 335302–335312.
5. Buesser, B.; Pratsinis, S.E. Morphology and crystallinity of coalescing nanosilver by molecular dynamics. *The Journal of Physical Chemistry C*. **2015**, *119*, 10116–10122.

6. Grammatikopoulos, P.; Cassidy, C.; Singh, V.; Benelmekki, M.; Sowwan, M. Coalescence behaviour of amorphous and crystalline tantalum nanoparticles: a molecular dynamics study. *Journal of materials science*. **2014**, *49*, 3890–3897.
7. Song, P.; Wen, D. Molecular dynamics simulation of the sintering of metallic nanoparticles. *Journal of Nanoparticle Research*. 2010, *12*, 823–829.
8. Johnson, R.A. Analytic nearest-neighbor model for fcc metals. *Physical Review B*. **1998**, 37:3924.
9. Lai, L.-F.; Lu, D.-M.; Hsu, K.-S.; Lu, J.-M. A Study of Nanoscale Vanadium Powder Applied on 3D Printing Process. Proceedings of IEEE International Conference on Knowledge Innovation and Invention, **2019**, 2019:142–144.
10. Lai, L.-F.; Lu, D.-M., and Lu, J.-M, Molecular Dynamics Simulation of Thermomechanical Properties of Hollow Palladium Nanoparticle Pairs during Additive Manufacturing, *Sensors and Materials*, 34(10), **2022**, 3911–3921.
11. Lai, L.-F.; Lu, D.-M. Chang, C.-M.; Su, Y.-C.; Hsu, K.S.; Lu, J.-M. Molecular Dynamic Simulation of the Thermomechanical Characteristics of Platinum Nanopowders during Additive Manufacturing Process. (to be appear)